

## Low-repetition-rate femtosecond operation in extended-cavity mode-locked Yb:CALGO laser

Dimitris N. Papadopoulos, Frédéric Druon, Justine Boudeile, Igor Martial, Marc Hanna, Patrick Georges, Pierre-Olivier Petit, Philippe Goldner, Bruno Viana

► **To cite this version:**

Dimitris N. Papadopoulos, Frédéric Druon, Justine Boudeile, Igor Martial, Marc Hanna, et al.. Low-repetition-rate femtosecond operation in extended-cavity mode-locked Yb:CALGO laser. *Optics Letters*, Optical Society of America, 2009, 34 (2), pp.196-198. hal-00533141

**HAL Id: hal-00533141**

**<https://hal-iogs.archives-ouvertes.fr/hal-00533141>**

Submitted on 30 Mar 2012

**HAL** is a multi-disciplinary open access archive for the deposit and dissemination of scientific research documents, whether they are published or not. The documents may come from teaching and research institutions in France or abroad, or from public or private research centers.

L'archive ouverte pluridisciplinaire **HAL**, est destinée au dépôt et à la diffusion de documents scientifiques de niveau recherche, publiés ou non, émanant des établissements d'enseignement et de recherche français ou étrangers, des laboratoires publics ou privés.



core diameter. By the addition of a  $q$ -preserving telescope, formed by a 2 m radius of curvature concave mirror and a plane one at a fixed distance of 1 m, we could easily vary the length of the cavity by properly choosing the number of beam bounces on the telescope mirrors [14,15]. Initially, the cavity round trip was set at 11 m, corresponding to two reflections on the concave telescope mirror. For the intracavity dispersion compensation we included 3 Gires–Tournois interferometer (GTI) mirrors with a group-velocity dispersion (GVD) =  $-550 \text{ fs}^2$  (Fig. 1). This resulted in a negative net dispersion that can be estimated around  $-2600 \text{ fs}^2/\text{round trip}$  (assuming  $\sim 50 \text{ fs}^2/\text{mm}$  for the CALGO crystal and  $0 \text{ fs}^2$  for all unknown dispersion optics: semiconductor saturable absorber mirror (SESAM), output coupler, dichroic mirror). The output coupler transmission was 5%, which corresponds to an optimum of intracavity power for the chosen GVD compensation. The SESAM (from Amplitude Système) has a modulation depth of 1% and a saturation fluence  $>120 \mu\text{J cm}^{-2}$ .

In this configuration the mode-locked regime was observed for an intracavity pulse energy between 0.3 and  $0.5 \mu\text{J}$ . The highest average power produced from this mode-locked laser was 650 mW at 27 MHz, corresponding to an output pulse energy of 24 nJ, for 16 W of pump power. Further increase of the output power resulted in an unstable mode-locking regime leading to cw operation; no multiple-pulse operation was observed. The pulse duration in this case was measured both with an autocorrelator and a second-harmonic generation (SHG) frequency-resolved optical gating (FROG) setup at 145 fs. The spectrum was centered at 1043 nm and had a bandwidth of 15 nm. The time bandwidth product is 0.6, and the FROG retrieved spectral phase of the pulse clearly indicates positively chirped pulses with a parabolic phase [Figs. 2(a)–2(c), left side]. These pulses, however, could be still used as direct inputs for various fiber amplifier systems [16,17].

Further increase of the intracavity dispersion to reduce the pulse duration directly out of the cavity made the mode locking of the oscillator impossible. Nevertheless, to compensate this parabolic phase of about  $3400 \text{ fs}^2$ , an external compressor based on a standard SF10 prism pair has been used. The compressed pulse duration is 93 fs. The corresponding SHG FROG trace and retrieved pulse shape and

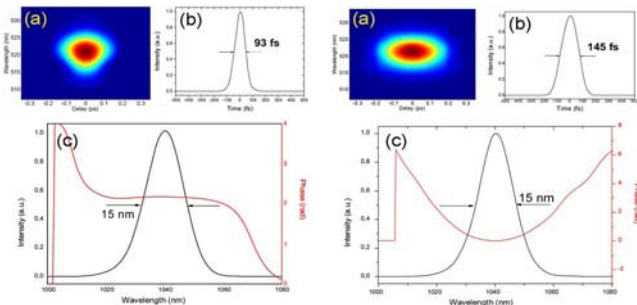


Fig. 2. (Color online) Pulse characterization at the output of the oscillator after (left) and before (right) compression. (a) Experimental SHG FROG trace, (b) retrieved pulse, (c) retrieved spectrum and spectral phase.

spectrum are shown in Figs. 2(a)–2(c) (right side). The time bandwidth product is reduced down to  $\Delta t \Delta \nu = 0.38$  while the main remaining spectral phase distortion is cubic. The values of the remaining phase is  $-140 \pm 5 \text{ fs}^2$  for the quadratic term,  $-6000 \pm 500 \text{ fs}^3$  for the cubic term and  $-1.4 \times 10^6 \pm 4 \times 10^5 \text{ fs}^4$  for the fourth order. The energy per pulse after compression is 17 nJ, corresponding to only 70% compression efficiency as a result of the reduced quality prisms used.

To further reduce the RR, we increased the cavity round trip to 20 m, adding two more round trips inside the telescope. For stable single-pulse mode locking the negative dispersion of the cavity had to be increased by adding two more GTI mirrors of  $-550$  and  $-250 \text{ fs}^2$  (about  $-4200 \text{ fs}^2$  net cavity dispersion). With this setup, the highest average power produced in the single-pulse regime was 240 mW at 15 MHz, corresponding to an output pulse energy of 16 nJ, for 13 W of pump power. The optimum output coupling of the cavity was 3.8%, corresponding to maximum intracavity pulse energy of  $0.42 \mu\text{J}$ . Further increase of the energy resulted in multiple-pulse instabilities [17–19]. In Fig. 3 the dependence of the output pulse duration as a function of the average output power is shown. We can clearly observe the onset of double pulsing for output power greater than 250 mW ( $\sim 16.5 \text{ nJ}$ ). The minimum pulse duration measured in this longer cavity with an autocorrelation and a SHG FROG setup [Figs. 4(a)–4(c)] was 170 fs. The spectrum was (for one or two pulses) centered at 1040 nm and had a bandwidth of 8 nm. The time bandwidth product for this spectrally narrower pulse is 0.37.

Modifying slightly the 27 MHz setup, it was also possible to observe double-pulse operation. In fact, increasing the intracavity energy and modifying the dispersion (replacing the left-most  $-550 \text{ fs}^2$  GTI in Fig. 1 with another one of  $\text{GVD} = -250 \text{ fs}^2$ , reducing the net dispersion to about  $-2000 \text{ fs}^2$ ), the soliton naturally splits in multiple pulses. Multiple-pulse operation is not unusual in femtosecond lasers [18–20], but in our case, owing to the very atypical dispersion curve of the cavity added to the very broad emission spectrum of the Yb:CALGO, it is possible to generate linearly polarized double pulses with different wavelengths, which we believe is the first demonstration of bicolor femtosecond double-pulse operation. Usually the multiple pulses are separated in time but not in the spectral domain. A very broad spectrum has been obtained with a bandwidth greater than 30 nm [Fig. 5(a)]. The spectrum can be almost perfectly fit with two Gaussian curves: one centered at 1040 nm

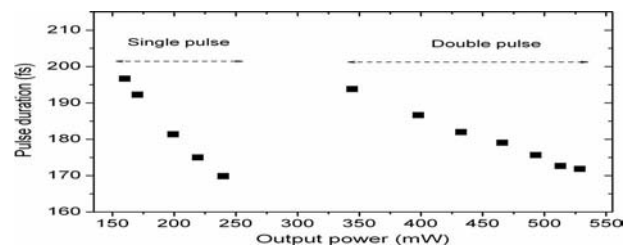


Fig. 3. Pulse duration as a function of the average output power for the 15 MHz laser cavity.

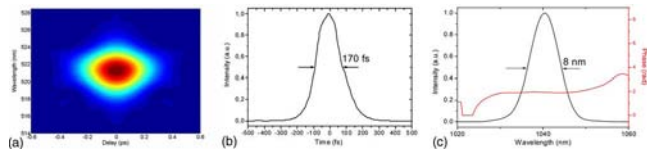


Fig. 4. (Color online) Pulse characterization at the output of the 15 MHz oscillator. (a) Experimental SHG FROG trace, (b) retrieved pulse, (c) retrieved spectrum and spectral phase.

with a bandwidth of 21 nm and one centered at 1057 nm with a bandwidth of 10 nm with lower amplitude ( $\sim 60\%$ ). This double pulse is clearly corroborated by the FROG exhibiting four spots forming a diamond shape [Fig. 5(b)]. Although the convergence of the retrieving algorithm from the FROG is low, we can evaluate the pulse durations to be respectively 80 and 130 fs with a pulse separation of 200 fs [Fig. 5(c)]. This bicolor double-pulse regime might be explained on the basis of the combination of two factors: first, the very broad and constant gain that, in the case of Yb:CALGO, is inhomogeneous owing to the contribution of its two different crystallographic sites  $Gd^{III}$  and  $Al^{III}$ , which allows one to reduce cross talk between the two pulses; second, and probably the most important effect, the specific intracavity dispersion distribution resulting in two spectrally distinguished regions of almost constant GVD, overlapping the two Gaussian contributions of the double pulse [inset of Fig. 5(a)].

In this Letter we demonstrated that it is possible to obtain sub-100 fs pulse at 27 MHz with a pulse energy of 17 nJ from an Yb-doped CALGO crystal. Further reduction of the RR down to 15 MHz has been also achieved, resulting in the generation of 170 fs pulses of 16 nJ energy directly out of the cavity. We also demonstrated an unprecedented bicolor double-pulse regime within a bulk oscillator generating ultrabroad bandwidth of about 30 nm. Two  $\sim 100$  fs pulses have been produced temporally separated by 200 fs and spectrally by 17 nm. This bicolor double regime is to our best knowledge an original observation. This regime is possible due to a very specific dispersion curve of the cavity with multiple inflexions,

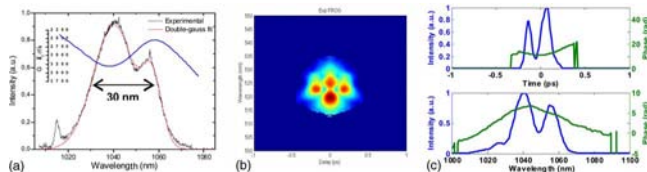


Fig. 5. (Color online) Dual-wavelength double-pulse operation regime. (a) Experimental spectrum and double Gaussian fit (intracavity GTI GVD as inset), (b) SHG FROG trace, (c) SHG FROG retrieved pulse temporal-spectral intensity and phase.

and this regime is probably helped by the broad and partly inhomogeneous gain of the Yb:CALGO, which tends to reduce cross-talk influence between the bicolor pulses.

## References

1. C. Honninger, F. Morier-Genoud, M. Moser, U. Keller, L. R. Brovelli, and C. Harder, *Opt. Lett.* **23**, 126 (1998).
2. F. Druon, S. Chénais, P. Raybaut, F. Balembois, P. Georges, R. Gaum, G. Aka, B. Viana, S. Mohr, and D. Kopf, *Opt. Lett.* **27**, 197 (2002).
3. F. Druon, S. Chénais, P. Raybaut, F. Balembois, P. Georges, R. Gaumé, P. H. Haumesser, B. Viana, D. Vivien, S. Dhellemmes, V. Ortiz, and C. Larat, *Opt. Lett.* **27**, 1914 (2002).
4. M. Tokurakawa, H. Kurokawa, A. Shirakawa, K. Ueda, H. Yagi, T. Yanagitani, and A. A. Kaminskii, in *Advanced Solid-State Photonics*, OSA Technical Digest Series (CD) (Optical Society of America, 2008), paper MG2.
5. V. Kisel, A. Troshin, V. Shcherbitsky, N. Kuleshov, V. Matrosov, T. Matrosova, M. Kupchenko, F. Brunner, R. Paschotta, F. Morier-Genoud, and U. Keller, *Opt. Lett.* **30**, 1150 (2005).
6. A. Schmidt, S. Rivier, V. Petrov, U. Griebner, A. Garcia-Cortes, F. Esteban-Betegon, M. D. Serrano, and C. Zaldo, *Electron. Lett.* **44**, 806 (2008).
7. A. Lucca, G. Debourg, M. Jacquemet, F. Druon, F. Balembois, P. Georges, P. Camy, J. Doualan, and R. Moncorgé, *Opt. Lett.* **29**, 2767 (2004).
8. Y. Zaouter, J. Didierjean, F. Balembois, G. Lucas-Leclin, F. Druon, P. Georges, J. Petit, P. Goldner, and B. Viana, *Opt. Lett.* **31**, 119 (2006).
9. R. Gaumé, B. Viana, D. Vivien, J. P. Roger, and D. Fournier, *Appl. Phys. Lett.* **83**, 1355 (2003).
10. J. Boudeile, F. Druon, M. Hanna, P. Georges, Y. Zaouter, E. Cormier, J. Petit, P. Goldner, and B. Viana, *Opt. Lett.* **32**, 1962 (2007).
11. S. V. Marchese, C. R. Baer, A. G. Engqvist, S. Hashimoto, D. J. Maas, M. Golling, T. Südmeyer, and U. Keller, *Opt. Express* **16**, 6397 (2008).
12. J. Neuhaus, J. Kleinbauer, A. Killi, S. Weiler, D. Sutter, and T. Dekorsy, *Opt. Lett.* **33**, 726 (2008).
13. T. Brabec, C. Spielmann, and F. Krausz, *Opt. Lett.* **17**, 748 (1992).
14. D. Herriott, H. Kogelnik, and R. Kompfner, *Appl. Opt.* **3**, 523 (1964).
15. D. N. Papadopoulos, S. Forget, M. Delaigue, F. Druon, F. Balembois, and P. Georges, *Opt. Lett.* **28**, 1838 (2003).
16. D. N. Papadopoulos, Y. Zaouter, M. Hanna, F. Druon, E. Mottay, E. Cormier, and P. Georges, *Opt. Lett.* **32**, 2520 (2007).
17. D. N. Papadopoulos, I. Martial, M. Hanna, F. Druon, and P. Georges, *Opt. Lett.* **33**, 1431 (2008).
18. V. L. Kalashnikov, E. Sorokin, and I. T. Sorokina, *IEEE J. Quantum Electron.* **39**, 323 (2003).
19. M. Lai, J. Nicholson, and W. Rudolph, *Opt. Commun.* **142**, 45 (1997).
20. M. J. Lederer, B. Luther-Davies, H. H. Tan, C. Jagadish, N. N. Akhmediev, and J. M. Soto-Crespo, *J. Opt. Soc. Am. B* **16**, 895 (1999).